AD-A252 684

‖‖‖‖‖‖‖‖‖‖‖‖‖‖‖‖‖‖‖

AFWAL-TR-85-1102

SEQAL DEFINITION STUDY: SYNTHETIC APERTURE RADAR IMAGE QUALITY METRICS

Science Applications International Corporation
1321 Research Park Drive
Dayton, Ohio 45432

JULY 1985

FINAL REPORT FOR PERIOD — MARCH 1982 - FEBRUARY 1985

DTIC
SELECTE
JUL 0 8 1992
S   D

Approved for public release; distribution is unlimited.

92-17551
‖‖‖‖‖‖‖‖‖‖‖‖‖‖‖‖‖‖
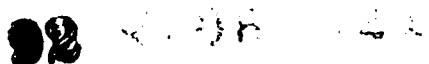
AVIONICS LABORATORY
AIR FORCE WRIGHT AERONAUTICAL LABORATORIES
AIR FORCE SYSTEMS COMMAND
WRIGHT-PATTERSON AIR FORCE BASE, OHIO 45433

NOTICE

When Government drawings, specifications, or other data are used for any purpose other than in connection with a definitely Government-related procurement, the United States Government incurs no responsibility or any obligation whatsoever. The fact that the government may have formulated or in any way supplied the said drawings, specifications, or other data, is not to be regarded by implication, or otherwise in any manner construed, as licensing the holder, or any other person or corporation; or as conveying any rights or permission to manufacture, use, or sell any patented invention that may in any way be related thereto.

This report is releasable to the National Technical Information Service (NTIS). At NTIS, it will be available to the general public, including foreign nations.

This technical report has been reviewed and is approved for publication.

WILLIAM L. FOLEY, GS-13
Project Engineer
WL/AARA-2
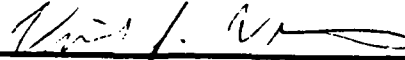
VINCENT J. VELTEN, GS-13
Actg Chief, Technology Group
WL/AARA-2
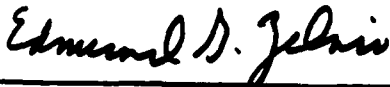
EDMUND G. ZELNIO, Acting Director
Mission Avionics Division

REPORT DOCUMENTATION PAGE

Form Approved
OMB No. 0704-0188

1. AGENCY USE ONLY (Leave blank)	2. REPORT DATE	3. REPORT TYPE AND DATES COVERED
	JULY 1985	FINAL REPORT; MAR 82 TO FEB 85

4. TITLE AND SUBTITLE	5. FUNDING NUMBERS
SEQAL DEFINITION STUDY: SYNTHETIC APERTURE RADAR IMAGE QUALITY METRICS	PE-62204F PR-7622 TA-08
6. AUTHOR(S)	WU-34 C – F33615-82-C-1825

7. PERFORMING ORGANIZATION NAME(S) AND ADDRESS(ES)	8. PERFORMING ORGANIZATION REPORT NUMBER
SCIENCE APPLICATIONS INTERNATIONAL CORPORATION 1321 RESEARCH PARK DRIVE DAYTON OH 45432	

9. SPONSORING/MONITORING AGENCY NAME(S) AND ADDRESS(ES)	10. SPONSORING/MONITORING AGENCY REPORT NUMBER
William L. Foley (513)255-1115 Avionics Laboratory (WL/AARA) Air Force Wright Aeronautical Laboratories Wright-Patterson Air Force Base, Ohio 45433-6543	AFWAL-TR-85-1102

11. SUPPLEMENTARY NOTES

12a. DISTRIBUTION/AVAILABILITY STATEMENT	12b. DISTRIBUTION CODE
Approved for public release; distribution is unlimited.	

13. ABSTRACT *(Maximum 200 words)*

THE WORK DESCRIBED IN THIS DOCUMENT ENCOMPASSED EFFORTS TO PROVIDE TO THE AIR FORCE WRIGHT AERONAUTICAL LABORATORY'S SENSOR QUALITY ANALYSIS LABORATORY (SEQAL) AN IN-HOUSE SYNTHETIC APERTURE RADAR (SAR) PERFORMANCE MONITORING AND MAINTENANCE PROGRAM FOR OPERATIONAL SAR SYSTEMS. THESE EFFORTS INCLUDED ADDITION OF DISPLAY EQUIPMENT AS WELL AS REHOSTED AND DEVELOPED SOFTWARE TO THE EXISTING FACILITY. THIS REPORT DOCUMENTS THE THEORETICAL AND ARCHITECTURAL DESIGN BACKGROUND FOR THE DISPLAY CALIBRATION AND INTERACTIVE IMAGE REMAPPING SOFTWARE WHICH WAS DEVELOPED, INSTALLED, AND TESTED IN THE SEQAL FACILITY.

14. SUBJECT TERMS	15. NUMBER OF PAGES
	53
	16. PRICE CODE

17. SECURITY CLASSIFICATION OF REPORT	18. SECURITY CLASSIFICATION OF THIS PAGE	19. SECURITY CLASSIFICATION OF ABSTRACT	20. LIMITATION OF ABSTRACT
UNCLASSIFIED	UNCLASSIFIED	UNCLASSIFIED	UL

FOREWORD

This technical report is submitted by Science Applications International Corporation as a summary of activities under the Statement of Work dated 26 February 1982. The work performed under this contract consisted, in part, of tasks to define the role and requirements for a Sensor Quality Analysis Laboratory (SEQAL) and was performed during the period from April - September 1982. That initial output is summarized in this report. The AFWAL project engineer during that period was Mr. Lloyd Clark. Later activities, between September 1982 and March 1985, consisted of software assessments, software conversion, integration and testing at SEQAL. The products of those tasks are also documented in this report. 1Lt John Hagood was the responsible AFWAL project engineer for those activities, and was the AFWAL lead engineer for SEQAL.

Accession For	
NTIS GRA&I	☑
DTIC TAB	☐
Unannounced	☐
Justification	
By	
Distribution/	
Availability Codes	
Dist	Avail and/or Special
A-1	

Table of Contents

List of Figures and Tables

FIGURES

TABLES

List of Acronyms

AFWAL   Air Force Wright Aeronautical Laboratory

ASARS   Advanced Synthetic Aperture Radar System

CRT   Cathode Ray Tube

DEC   Digital Equipment Corporation

FFT   Fast Fourier Transform

IO   Information Office

IOC   Initial Operational Capability

IPR   ImPulse Response

ITT   Intensity Transformation Table

LUT   LookUp Table

NTIS   National Technical Information Service

OFM   Output Function Memory

RMS   Root Mean Square

SAIC   Science Applications International Corporation

SAR   Synthetic Aperture Radar

SEQAL   Sensor Quality Analysis Laboratory

TNR   Terrain-to-Noise Ratio

USAF   U. S. Air Force

VOC   Video Output Controller

I. INTRODUCTION

Background

The Sensor Quality Analysis Laboratory (SEQAL) represents the first opportunity for the USAF to establish an in-house Synthetic Aperture Radar (SAR) performance monitoring and maintenance program for operational systems. Previous and current operational SAR systems have had: (1) no standardized definitions of performance quality; (2) no standard method regularly used to quantify actual performance; and (3) no documented way to diagnose poor performance quality beyond normal field maintenance manuals. While this has been unnecessary for the current situation with only a handful of SAR equipments, this lack of standardized testing and evaluation will be unacceptable for the future.

The number of operational SAR imaging systems will increase dramatically over the next few years. UPD-4 systems are currently being manufactured for both the USAF and the Marine Corps, the TR-1 is rapidly approaching deployment, and other high performance SAR systems are being developed. Thus, within the next few years, there will be more systems in the field built by different contractors, with new and sophisticated SAR modes. It is vitally important that the USAF establish an in-house (independent from the SAR manufacturers) capability to provide SAR image quality measurement methodologies and tools to support these systems.

A decade ago, just the ability to make a "photo-like" radar image of the ground from an operational reconnaissance aircraft was considered quite an accomplishment, and if the imagery could be used to perform some reconnaissance functions in night and all weather conditions the user was generally satisfied. The "handbook" method of measuring radar performance, i.e., the ability to resolve point reflectors on the ground, was the accepted method for determining the SAR's performance.

During the past few years since SAR systems have been in operational use, two general classes of historical developments have occurred which have demonstrated that simple resolution measurements are inadequate to characterize SAR image quality. The first of these has been the experience gained in using both operationally collected imagery and that collected experimentally. As operational systems were applied to increasingly subtle reconnaissance tasks, it became evident that factors other than resolution were affecting the utility of the imagery. Target "swallow", sidelobes, and signal-induced noise effects were substantial contributors to image quality degradation. At the same time these real world observations were being made, analytical models were being developed to predict and to quantify the impact of various effects on image quality. Therefore, the time is ripe for real world observations to be coupled with analytical understanding to provide the required foundation for standardized SAR image quality analysis and for improvement when the image falls out-of-bounds. This is especially necessary, since for the first time, the SAR systems under development

1

have specific and quantified elements of image quality in their development specifications.

Some Image Quality Elements

As a result of field experience with SAR systems, the analytical work performed over the past decade has resulted in a more comprehensive set of image quality metrics than previously existed. These metrics go well beyond the classical resolution performance used in quantifying the real quality of a SAR image. These image quality measures include:

- System Impulse Response (IPR)
- IPR Sidelobe Levels
- Image Contrast Ratios (terrain-to-noise ratio)
- Image Intensity Fidelity (including linear dynamic range and small target suppression)
- Image Artifacts
- Geometric Distortion
- Image Intensity Uniformity

Each of these elements of image quality can be perturbed by one or more components of the SAR system.

Generally, image Quality specifications have not been complete, either from the standpoint of all image quality factors or of a complete system chain to the output device; however, relative to the UPD-4, recent SAR systems have made a quantum leap in image quality specification.

The data for quantifying image quality parameters or related problems in a specific SAR system can come from several points in the signal processing chain and can be in several forms:

- Unprocessed Phase History Data (digital data)
- Processor Output Imagery (digital data or hardcopy imagery)
- Softcopy Displays (CRT)

A Historical Synopsis of SAR Image Quality

Initial SAR systems were almost exclusively dedicated to demonstrating constantly improving resolution. Specifications included only top level parameters and did not specify the complete radar product chain as represented at the output film or display. As resolution capabilities were improved, the importance of system instabilities and nonlinearities on signal-induced noise became evident. The use of error budgets during radar design became an important tool for controlling the design to meet image quality. Extensive evaluations were made with initial high resolution SAR imagery to develop image utility factors and radar interpretation

2

keys. New studies and analyses have shown the importance of extending the image quality chain through the radar output devices. However, most image quality drivers have yet to be fully understood or measured in controlled tests.

Image quality analysis has historically been IPR and/or sidelobe related. The definition and analytical appreciation of both a complete parametric set and a complete system chain of image quality factors is just now emerging.

Historically, image quality measurement techniques have lagged far behind both the level of analytical understanding and technological capability. Typically, the programs have been well into operational use before significant measurements are conducted. The ASARS-2 may be the first exception to this pattern.

Image quality evaluation is the cornerstone on which to base meaningful image quality trade-offs. It made a significant stride forward with Avionics Laboratory (AFWAL/AA) assistance in the mid 70s. Much data, however, is limited by the intrinsic system design of the initial Spotlight radar. The use of ASARS data is expected to show, for the first time, the effects of controlled, signal-induced noise in improving image utility.

Current Image Quality Planning

Current SAR programs have defined image quality specifications. These specifications will presumably be validated during initial system testing. Planning for post-IOC image quality testing and maintenance for these programs is sketchy at best. The sensor operators have no published plans for institutionalized image quality maintenance. Other developmental SAR systems indicate planning in this area may start "next year". In all cases, the development program offices are too occupied with developmental "issues" to worry about post-IOC problems.

It is apparent that no specific procedures or equipment have been planned for image quality monitoring. Because of the relatively recent definition of image quality parameters and the R&D nature of their application to date, no one has given real thought to adapting the parameters and their measurement to real-world operational programs. Thus, an independent laboratory such as AFWAL/AA can potentially fill an important void in several current SAR programs. What is needed, therefore, is an approach or methodology to get started.

The AFWAL/AA Approach to SEQAL

SAIC recommended a four-phase SEQAL development approach outlined below. This technical report, resulting from this recommendation, discusses the task areas and contractor support provided for Phases 0, I and II. Task areas and support for Phase III are deferred until specific SAR program involvement has been realized.

3

Phase 0: Objectives Baselining

In Phase 0, a Statement of Objectives was prepared as the vehicle for establishing funding lines and technical interfaces for an initial commitment between Government agencies.

Phase I: Definition and Program Planning

A tentative Phase 0 commitment led to the Phase I Definition and Program Planning effort. The Phase I products included:

1) An evaluation of image quality measurement techniques

2) A SEQAL Development Plan (tasks, work flow, costs)

3) An initial architecture and design for the equipment installation and facilities modification

Phase II: Implementation of Software Image Quality Metrics

The Phase I efforts led to tasks to rehost existing image quality software packages onto the SEQAL computer facility. Procedures and software were developed to calibrate and linearize the SEQAL facility displays, and to perform interactive image remapping functions. The software packages were installed and initially evaluated.

This report summarizes the key technical issues addressed during this phase of the program.

Phase III: Operations

The Phase II results will be reviewed to confirm the direction and scope of activities for Phase III, Operations. In Phase III, SEQAL resources will be used to measure and demonstrate the effectiveness of the image quality evaluation techniques using operational data. Phase III initial products will include:

1) A validated SEQAL Image Quality Evaluation Plan and Procedures

2) A SEQAL Performance Evaluation Report

3) A validated SEQAL Training Package

These initial operational results will be reviewed to establish the scope of subsequent full scale operational activities, including a determination of which operational systems will be monitored using SEQAL.

II. SYSTEM DEVELOPMENT SUPPORT ACTIVITIES

Introduction

The Sensor Quality Analysis Laboratory (SEQAL) was developed by the Air Force Avionics Laboratory Sensor Evaluation Branch (AARF) to provide the government with an in-house capability to evaluate sensor performance. The original work on SEQAL was performed in response to a requirement for the evaluation of Synthetic Aperture Radar (SAR) image quality (IQ). A SAR signal may pass through several stages between the radar and the final image. In each of these stages the image quality may become degraded. The objective of SEQAL was to track the image through the system to determine where image degradation took place. Science Applications International Corporation (SAIC), a leader in SAR analysis, assisted in the development of this capability.

An initial concept was to use SEQAL for the close support of a major classified system development. This concept was not pursued due to programmatic reasons, but is still considered technically viable. This section of this report sets out the approaches used in role definition, requirements definition, and the resulting SEQAL definition.

SEQAL Role Definition

If SEQAL were to support SAR technology programs and system development, it was necessary to determine the role the Avionics Laboratory should seek for it. The approach selected was to use SEQAL as an off-line diagnostic tool. The initial program support would begin during the integration phase of a program, with SEQAL providing assessment of the design through demonstration of design trade-offs affecting system transfer functions.

As a second follow-on phase, SEQAL would provide segment and system verification which would confirm product performance and system integration through actual measurements on the SAR system. This phase would actually measure image quality using Impulse Response (IPR) scans of imagery (on either film or high density tape), Root Mean Square (RMS) noise evaluation, and terrain-to-noise ratio (TNR) evaluations. These measurements would be performed on the overall system on a daily to monthly basis and at the segment level on a daily to weekly basis.

A third phase would continue during actual operation of the complete system providing an assessment of product performance compared with standards, and giving an evaluation of the sources and extent of image quality degradation.

SEQAL Requirements Definition

With the of the role of SEQAL in support of system development established, the next major step was to define requirements for SEQAL. It was decided that all requirements should be traceable from the operational system back through the

implementation and design phases to the original requirements definition. Figure 1 shows SEQAL requirements traceability flow.

Documentation Review

In late spring of 1982 SAIC reviewed available documentation on system test and integration in order to establish a baseline for SEQAL support.

This review disclosed that, although the procedures and schedules for system testing are being clearly defined, very few test criteria are included in the various test plans. It was also discovered that very few planned measurements could be directly related to the system level specification; thus traceability upward from test to system requirements was indirect.

Due to the lack of test criteria and the variability of measurement criteria it was decided that the test signals should be designed to test the needs of each segment and subsystem wherever possible. A further restriction is imposed by the requirement that no part of the system would require any special configuration of equipment to match the signal. It was determined that certain test signals could be qualitative. Measurement criteria can be established which define constant measurement points in both the linear and non-linear signal path. It was further determined that measurement results should be readily interpreted and should uniformly represent the system.

SEQAL Definition

With both the SEQAL role and the SEQAL requirements established, it became possible to delineate a meaningful SEQAL definition. The final SEQAL definition was predicated upon four major precepts: (1) the importance of image quality verification, (2) the SEQAL concept for support during test and integration, (3) an approach for continuous thread signal and diagnostics, and (4) the AFWAL commitment to SEQAL. The following paragraphs examine each of these areas briefly.

It is envisioned that SEQAL can provide image verification not only during system development, but could continue to provide image verification after system IOC. During the pre-IOC phase properly designed test signals could define image quality at the input and output ports of the various segments of the system. System end-to-end tests could also be performed to allow overall evaluation of the system transfer function. Precise measurement and diagnostic tools would enable developers to assess image quality continuity against specifications.

In the post-IOC phase, SEQAL could evaluate system degradation and could help isolate the degradation source. It could also provide the measurements and diagnostic tools to evaluate monitored live data.

A major concept which resulted from this SEQAL definition was the "continuous thread" test concept. In continuous thread testing a single known signal is tracked and measured during its passage through the system. Since the signal parameters at the system input are known, it becomes possible to evaluate

SEQAL Requirements Definition

System Support Requirements

Interface Requirements

Functions

Performance

Test

SEQAL Design Phase

Hardware/Software Architecture Design (Mods)

Test Specification

Interface Agreements

Hardware/Software Development

Interface Specifications

Hardware/Software Interface Specification

SEQAL Implementation Phase

Hardware Modification Plan Software Development Plan

System Test Plan

SEQAL Operations

Operations Plan

Figure 1: SEQAL Requirements Traceability

7

the transfer function for each segment of the system as well as for the overall system. This allows one to pinpoint critical points in the system where signal degradation may occur. Based on this continuous thread signal approach, diagnostics for a specific system can be developed and applied to monitor the image transfer quality throughout the system.

The AFWAL/AARF charter developed throughout the above was to measure image quality at various points in the image chain, to diagnose sources of error to the segment level in the system, to support integration and testing, and finally to support systems operation.

III. DISPLAY CALIBRATION TECHNIQUE DEVELOPMENT

Background

The response of the SEQAL DeAnza IP8500 has been measured. This data provides a basis for controlling the response through the use of compensation look-up tables (LUTs). The IP8500 users can obtain the desired response curve for simulating an imaging system, optimizing image utility, or for repeatability. They can use a look-up table which defines the CRT response and, after obtaining the desired image, use a second look-up table to duplicate the appearance of that image on film.

This report contains the uncorrected response curves as well as look-up tables for producing a linear response. A program listing was separately provided which can be used to produce a look-up table from the uncorrected data. This look-up table may be placed either in the memory channel Intensity Transformation Tables (ITTs) or the Video Output Controller (VOC) Look-Up Table. It is preferable that the VOC LUT be used since this will affect all memory channels assigned to it. Thus, the correction data need only be stored in one LUT vs. each ITT. This leaves the ITTs free to contain other response curves (e.g. square-law or logarithmic).

The computer program CALIBRATE contains data for the IP8500 CRT response. A user need only run CALIBRATE data tables. Look-up tables are provided here for illustrative purposes and need not be entered manually as long as CALIBRATE is available.

Methodology

The variety of possible CRT display control settings provides a large number of response curves without necessarily allowing the selection of a desired response characteristic (Figure 2). In order to generate the desired response, a standard set of control positions must be chosen, the response must be measured, and a compensation table must be generated (Figure 3).

The response curve is measured by commanding a uniform grey level (0 - 225) across the CRT screen and measuring the brightness or reflectance. A photometer with a spectral response similar to that of the human eye is used for measuring light levels. The temporal stability should be within one grey level (~0.4%) throughout the time required to generate a response curve. This has been verified for the CRT display by monitoring the output without changing the commanded grey level (grey level 127 in Figure 4).

Figure 5 illustrates the display response and the corrected straight line response for the IP8500. A brightness control setting of 6.58 was used to obtain this response. Note the effect of brightness control backlash. The 6.58 position should be set by turning the knob to the left (counter-clockwise). The correct brightness control setting is most accurately achieved by commanding grey level zero across the entire screen. Then, with the room lights out, adjust the screen

9

Note: No Significant Gain In Linearity Is Achieved By Trading Contrast Dynamic Range. Therefore, 100% Contrast And Grey Level Compensation Tables Should Be Used
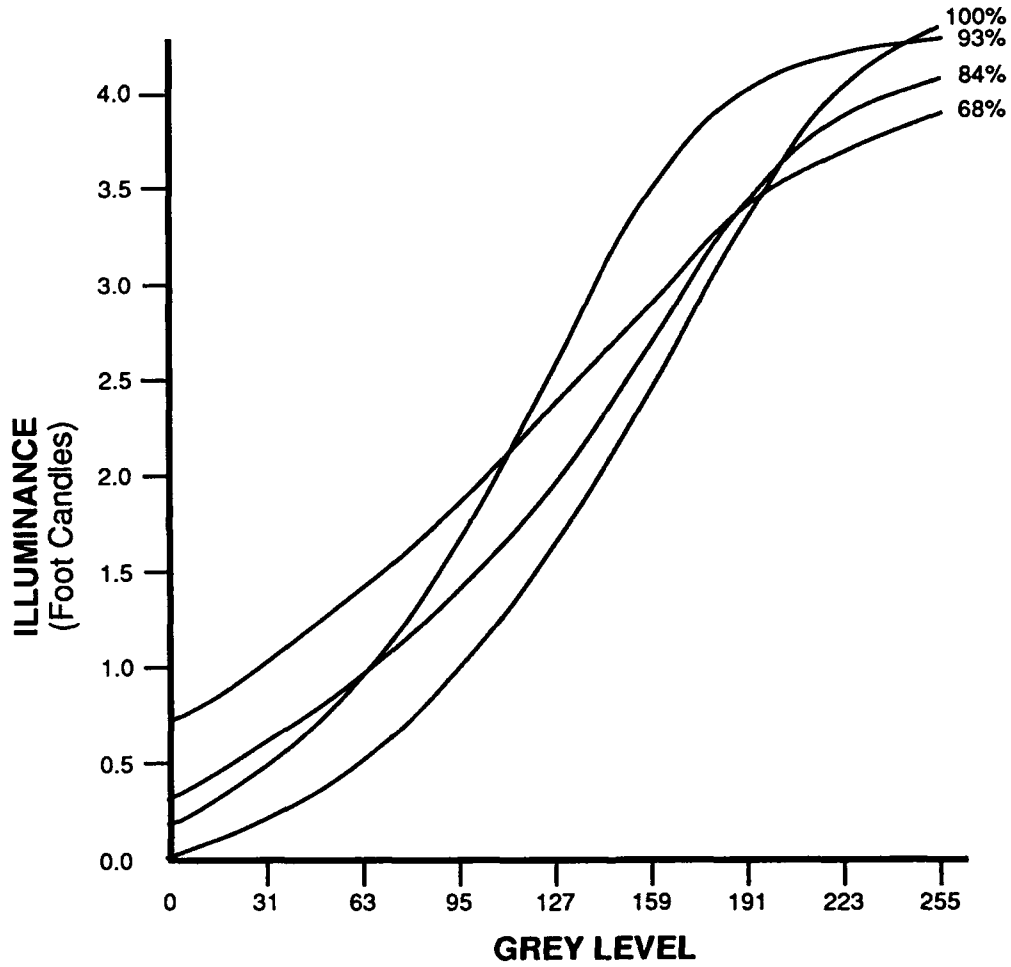
Figure 2: Contrast Versus Linearity Tradeoff

A. Measure Response
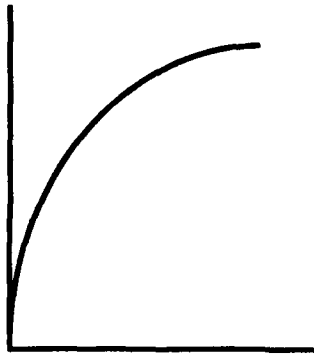
B. Generate Compensation
Table

measured
response

desired
response
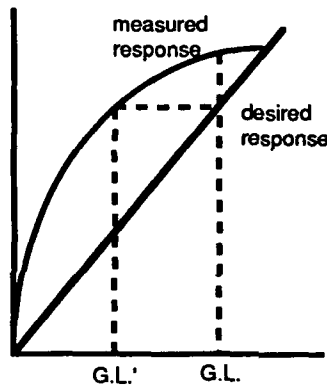
$F(G.L.) = f(G.L.')$
where f is measured
response and F is
compensated response

G.L.'   G.L.

C. Apparent Response with
Compensation Table
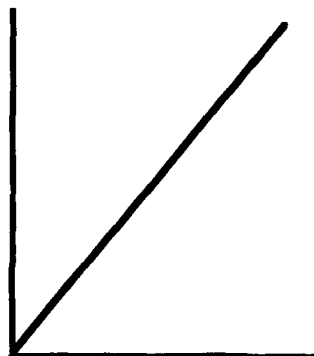
Figure 3: Compensation Table Generation

11
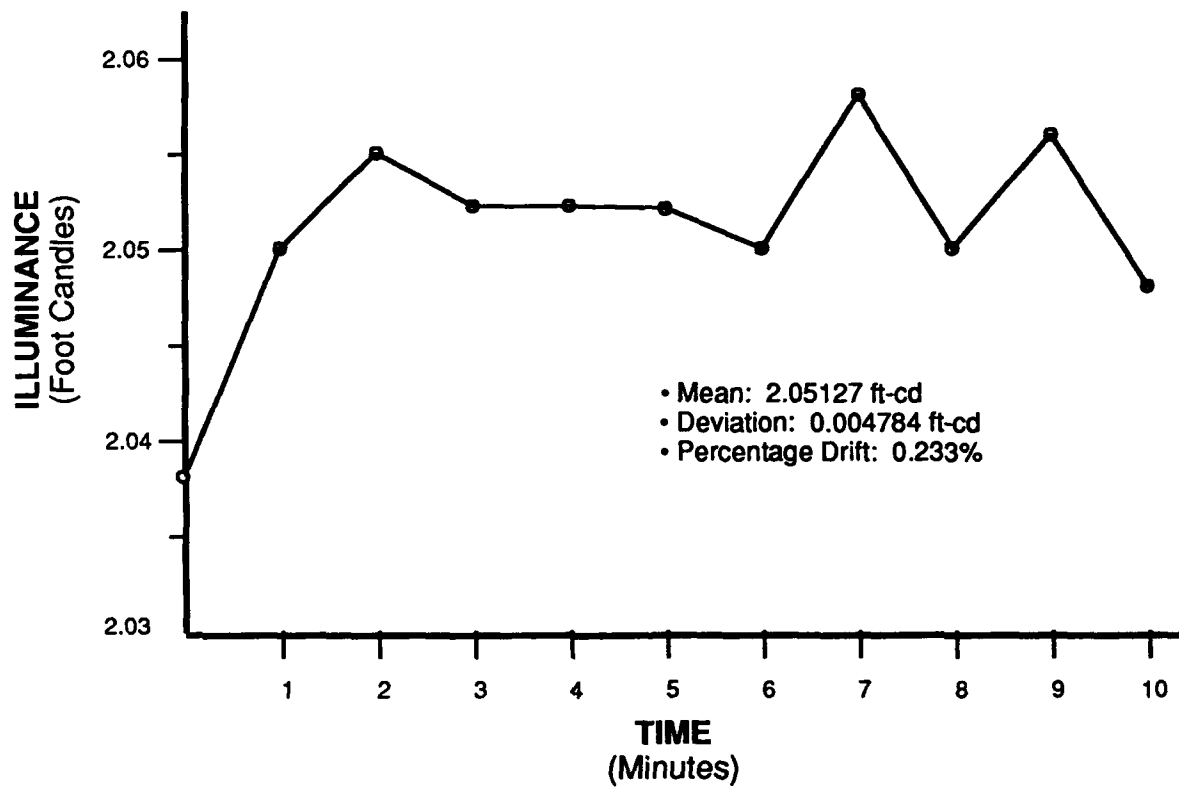
Figure 4: Temporal Stability
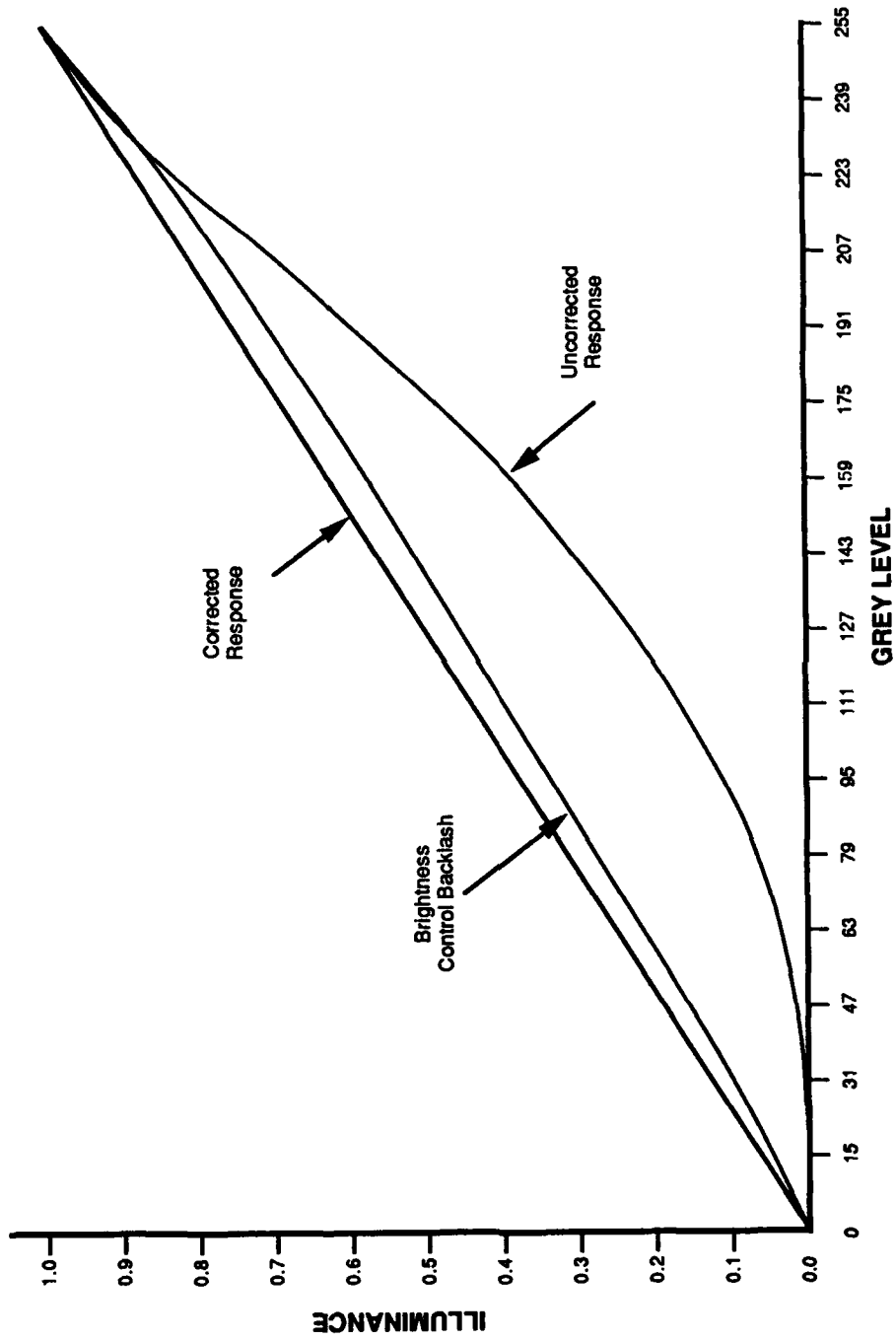
Figure 5: CRT Response

brightness so that the bright edges just disappear into the background. At this time the internal gain control does not yet have a calibrated scale. The gain control is relatively inaccessible and should not be tampered with until a scale setting can be published. Figure 6 portrays the illuminance curves for the display.

Table I contains normalized response data for the CRT display. The corrected data yields a straight line within the unavoidable errors of grey level quantization and CRT drift.

Table I: CRT Response

GREY LEVEL	UNCORRECTED	CORRECTED		IDEAL
		Set Dial		
		6.58 Left	6.58 Right	
0	0	0	0	0
15	.00141			
31	.00565	.123	.0975	.122
47	.0183			
63	.0388	.248	.213	.247
79	.0692			
95	.111	.373	.337	.373
111	.164			
127	.227	.500	.454	.498
143	.303			
159	.389	.623	.577	.624
175	.486			
191	.593	.747	.703	.749
207	.704			
223	.823	.872	.837	.875
239	.924			
255	1.00	1.0	1.0	1.0
Illuminance one foot from the screen at Grey Level 255	3.94 ft-cd	4.08 ft-cd	3.93 ft-cd	
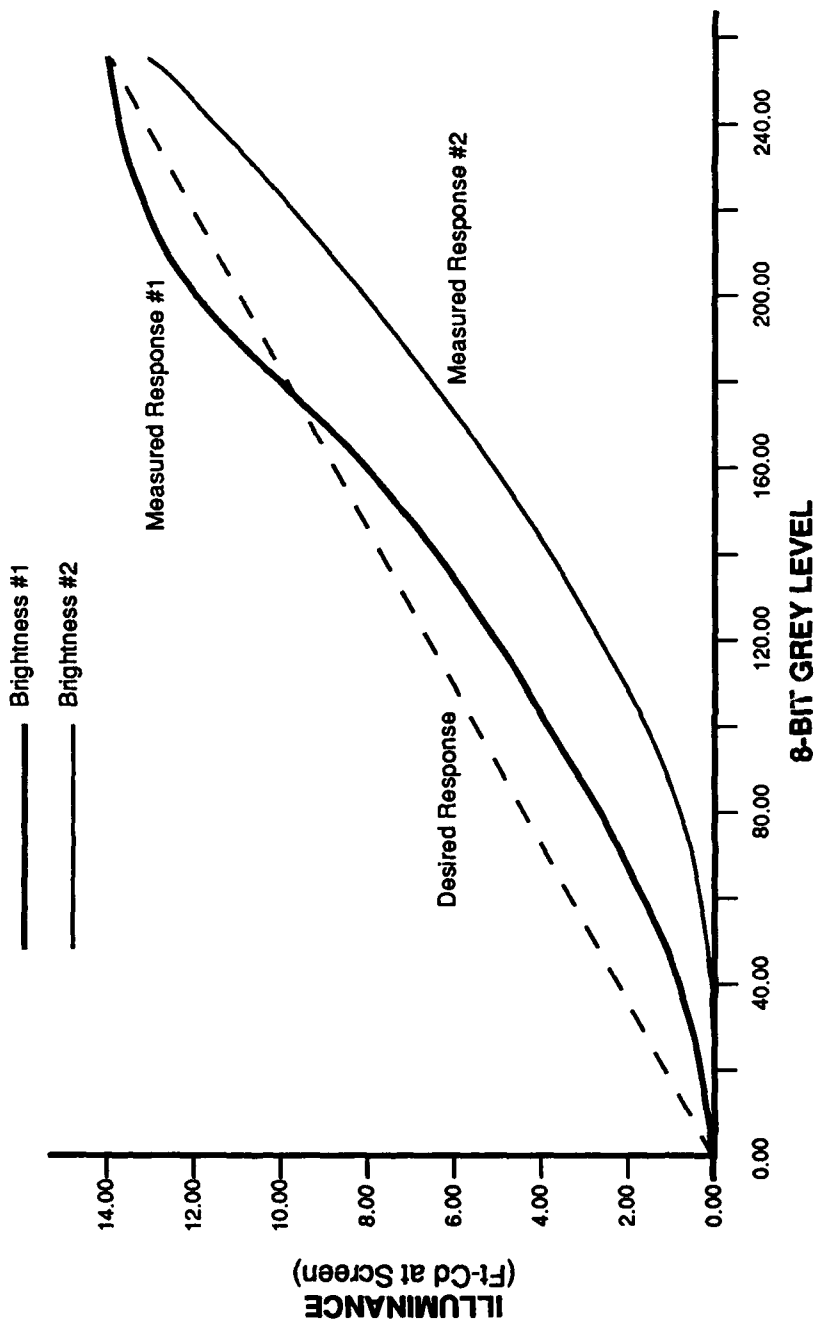
Figure 6: Illuminance Curves

15

Photometer Hardware Design

A combination of an optical filter, photovoltaic detector, and operational amplifier is used to produce a voltage output which is a linear function of light input over about eight orders of magnitude.

The classical diode equation describes the behavior of the photovoltaic p-n junction in the absence of light:

$$I_{dark} = I_o(e^{qv/kt} - 1) \qquad (1)$$

where the dark current (I_{dark}) is a function of the reverse saturation current (I_o), the electronic charge (q), the voltage appearing across the junction (V), Boltzmann's constant (k) and the absolute temperature (T). Figure 7 illustrates how the diode curve is shifted in the presence of light by the photocurrent:

$$I_p - \eta qEAd \cdot \frac{\lambda}{hc} \qquad (2)$$

where η is the quantum efficiency, E is the irradiance (watts/cm^2), Ad is the detector area, λ is the light wavelength, h is Planck's constant, and c is the speed of light. The total current in the presence of light is:

$$I_{light} = I_o(e^{qv/kt} - 1) - \eta qEAd\frac{\lambda}{hc} \qquad (3)$$

The short circuit current (that is, for V=0) is just the photocurrent of equation (2). The short circuit current is, therefore, a linear function of irradiance. However, the exponential in equation (3) indicates that the open circuit voltage is not a linear function of irradiance:

$$V_{oc} = \frac{kT}{q} \ln\left[\frac{I_p + I_o}{I_o}\right] \qquad (4)$$

Therefore, we will operate the detector into a virtual short circuit as a current source in order to obtain a linear output as a function of irradiance. This is accomplished using the transimpedance amplifier circuit of Figure 8. The output voltage is the product of the photocurrent and the feedback resistance which is linear in irradiance:

$$V_o = I_pR_f = \eta qER_fAd\frac{\lambda}{hc} \qquad (5)$$

The photometer must be able to measure illuminance (foot-candles) to provide meaningful data for a display which will be used by the human eye. An optical filter is required such that the detector response convolved with the filter response duplicates the photoptic response of the human eye. An integrated filter-detector
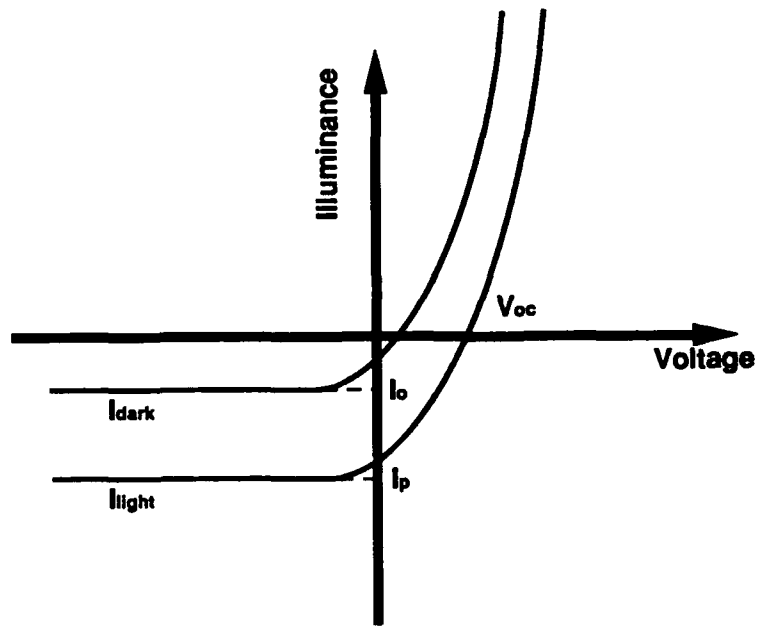
FIGURE 7: Photovoltaic I (V) Characteristic
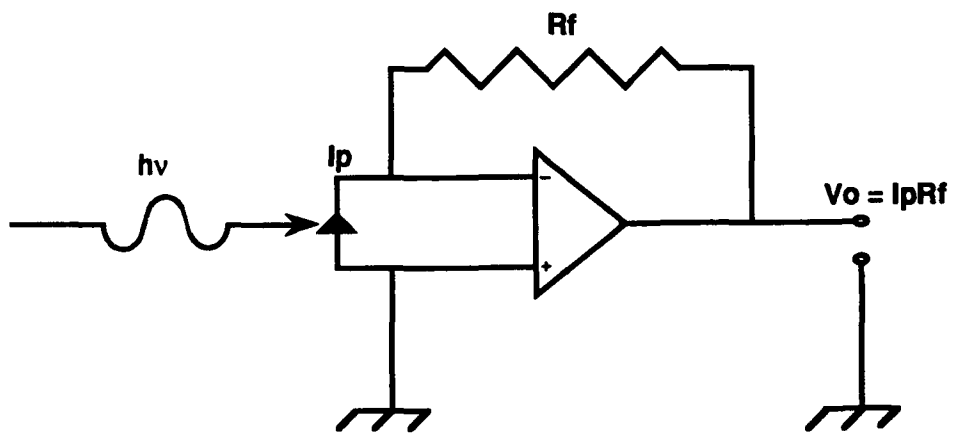
Figure 8: Transimpedance Amplifier Circuit

package (Silicon Detector Corporation SD 444-44-12-263) which provides this characteristic is used. The output response of the actual device used is then:

$$V_o = \int_{380nm}^{780nm} \eta q \frac{E_v}{k(\lambda)} R_f A d \frac{\lambda}{hc} d\lambda \tag{6}$$

where E is the illuminance in ft-cd (lumens per square foot), $k(\lambda)$ is the photoptic spectral luminous efficacy (lumens per watt), and Ad is now measured in square feet. A numerical integration of equation (6) need not be performed, because the manufacturer has determined that the photoptic response of the detector-filter combination is 0.36 A per ft-cd. The resistor used for R_f is a 1% precision metal film 100,000 ohm resistor. Therefore:

$$V_o = 0.36 \times 10^{-6} \text{ A/ft-cd} \times 10^5 \Omega$$

$$= 3.6 \times 10^{-2} \text{ volts/ft-cd} \tag{7}$$

Alternately, given a voltage reading V, the illuminance in foot-candles is:

$$E_v = 27.778 \text{ V} \tag{8}$$

Compensation Table Calculation

A simple procedure is used to calculate compensation look-up tables. The method was developed by Mike Cannon of Los Alamos (505-667-3797). The calibration program uses a spline curve-fitting subroutine to interpolate between grey-levels for which there is measured data. The program gives the user the option of placing the compensation table into any or all of the IP8500 ITTs or the VOC LUT. If the table is placed in the Output Function Memory (OFM), the user can state the number of channels to be added together (up to 3) for the correct scaling of the VOC LUT.

IV. INTERACTIVE IMAGE REMAPPING TECHNIQUE DEVELOPMENT

Introduction

Task B of the contract provided for the rehosting of image display remapping software (developed by the SAIC image processing facility in Tucson), from an International Imaging Systems processor to SEQAL's DeAnza IP8500 system. Both SAIC Tucson and SEQAL use DEC VAX computers as host for their image processors.

This section of the report provides a general description of the remapping software along with remapping algorithms, program capabilities, operating instructions, and the relationship of the software to the DeAnza IP8500 architecture. Large sections of the original informal report (1984 July 25), written by C. Cotter, M. Price, and J. Zelenka of the SAIC, Tucson facility, were used in this report.

Program Description

The objective of the REMAP software is to transform digital image data with bit-widths greater than 8 bits to an 8-bit representation that will optimize the interpretability of the image.

Originally, data is collected from an imaging type sensor and processed into a digital representation of the picture elements (pixels) of the image. A log-compression operation is used to reduce the number of bits required for the representation in order to conserve signal bandwidth for transmitting the data from the sensor platform to the ground station. The amplitude data bit-width is also wider than the 8-bit word widths of most digital image processors.

The log-compressed data is then decompressed to the original amplitude representation and then "remapped" or transformed into another 8-bit representation by a power law remapping algorithm. The remapping algorithm permits the operator to interactively vary the contrast and brightness of an image, in order to enhance the interpretability of the image content and to allow a CRT display to mimic a film and light table display of the image. The "remapped" image can then be displayed on a CRT or sent to a laser-beam film recorder, where a laser writes pixels on film in much the same way as the electron beam controls image intensities on a CRT screen.

Continuing the analogy comparing this digital approach to film storage and display, film transmittance in the film duplicate positive (complementary of a negative) correlates with brightness in the original scene. The brightest areas of an image appear opaque on a negative, but clear on a positive. Clear areas allow the transmission of energy (high transmittance) and appear brightest to an observer when light is passed through a positive and observed on a light table. Film transmittance of a duplicate positive and display brightness are thus analogous. Furthermore, the amount of light transmitted through a negative or positive

19

depends on the density of deposited metallic silver in the image. The differences in density values define the contrast of the image.

Figure 9 is a functional block diagram depicting the remapping of amplitude data to either a hard-copy laser-beam film recorder or to a softcopy CRT display. The remapping formula relates amplitude data, A, to input counts, C, to a film recorder. It derives the input counts in terms of the average film density amplitude statistics over the histogram of the image, and the amplitude value for that pixel location. The remapping part of this section gives the derivation of this transformation. In terms of the DeAnza architecture, the remapped values are stored on the ITT, or Intensity Transformation Table, where each pixel value on the memory channel is used as an index into an array location that contains the remapped value. (Figure 10 gives a general diagram of the DeAnza architecture.)

For softcopy displays, the input count to the film recorder, C, is related to the CRT drive voltage by means of the DeAnza Secondary Look-up Table (see Figure 10). The Secondary Look-up Table is loaded at the beginning of the program. Values are calculated by equating CRT brightness with film transmittance and using the knowledge of how the drive voltage controls the screen brightness, as set forth in the part of this section relating film-recorder inputs to display inputs.

After invoking an image on the display and selecting a region of interest, the user can interactively change parameters which, under program control, modify the contrast and/or the average log of the displayed brightness. As these parameters are changed, the ITT is updated and the remapped image is displayed. The user changes these values until the image is at maximum interpretability, then depresses 'ENTER' to indicate the remapping is complete.

Remapping

This section gives the derivation for the formulas used to relate amplitude data to the input counts going to a hard copy laser beam film recorder. There are two sets of remapping functions. Each of these will be presented in turn.

The transformation from image amplitude to transmittance on the duplicate positive is a power law remapping of the general form:

$$T = TMIN \qquad \text{for} \quad A \leq A0$$

$$T = TMAX \left(A/ASAT\right)^P \qquad \text{for} \quad A0 \leq A \leq ASAT$$

$$T = TMAX \qquad \text{for} \quad ASAT < A$$

where:

- T is the film transmittance value of the duplicate positive

- TMIN is the minimum film transmittance value

- TMAX is the maximum film transmittance value

20
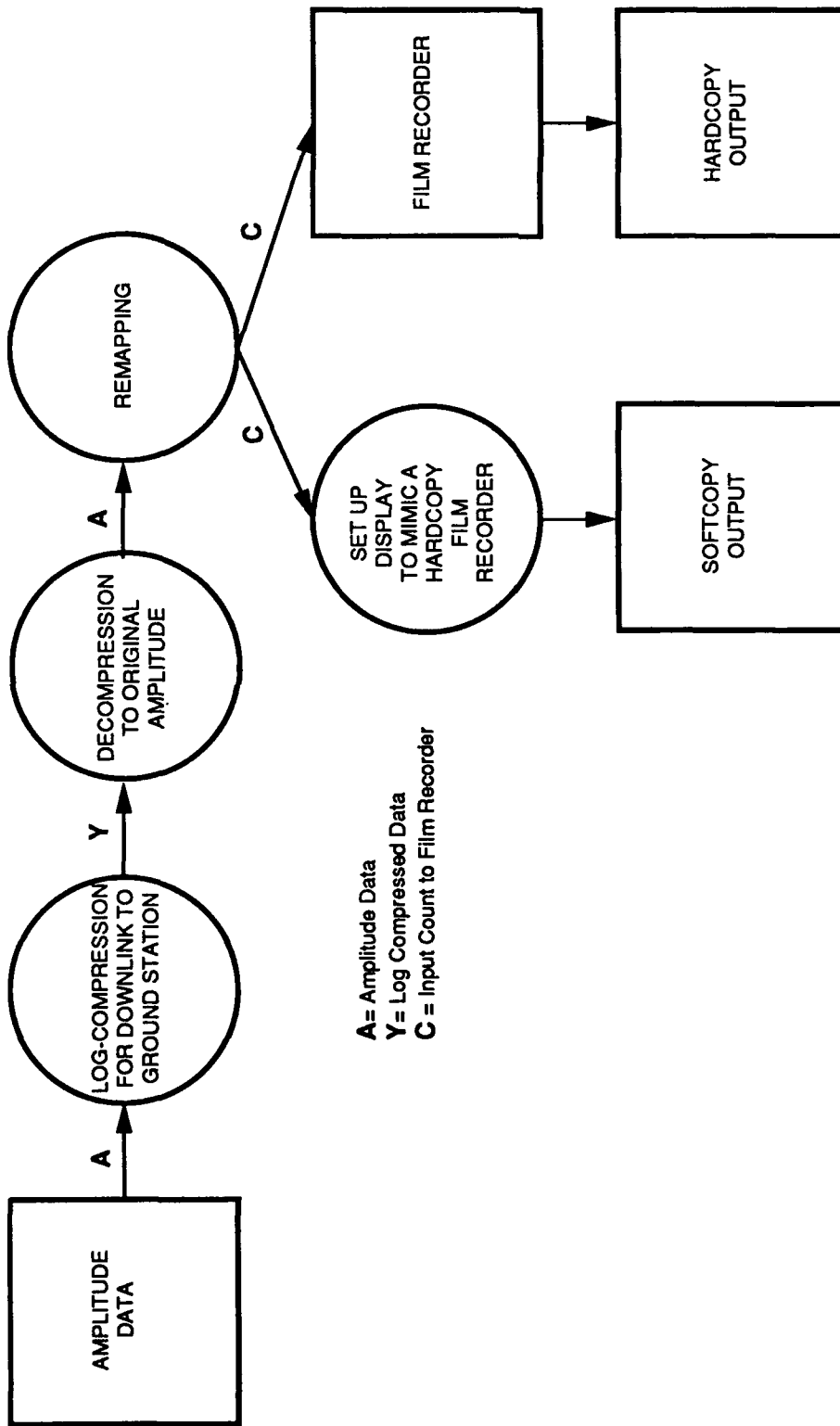
Figure 9: Remapping Process Diagram

AMPLITUDE DATA

A

LOG-COMPRESSION FOR DOWNLINK TO GROUND STATION

Y

DECOMPRESSION TO ORIGINAL AMPLITUDE

A

REMAPPING

C

C

FILM RECORDER

HARDCOPY OUTPUT

SET UP DISPLAY TO MIMIC A HARDCOPY FILM RECORDER

SOFTCOPY OUTPUT

A= Amplitude Data
Y= Log Compressed Data
C = Input Count to Film Recorder

21
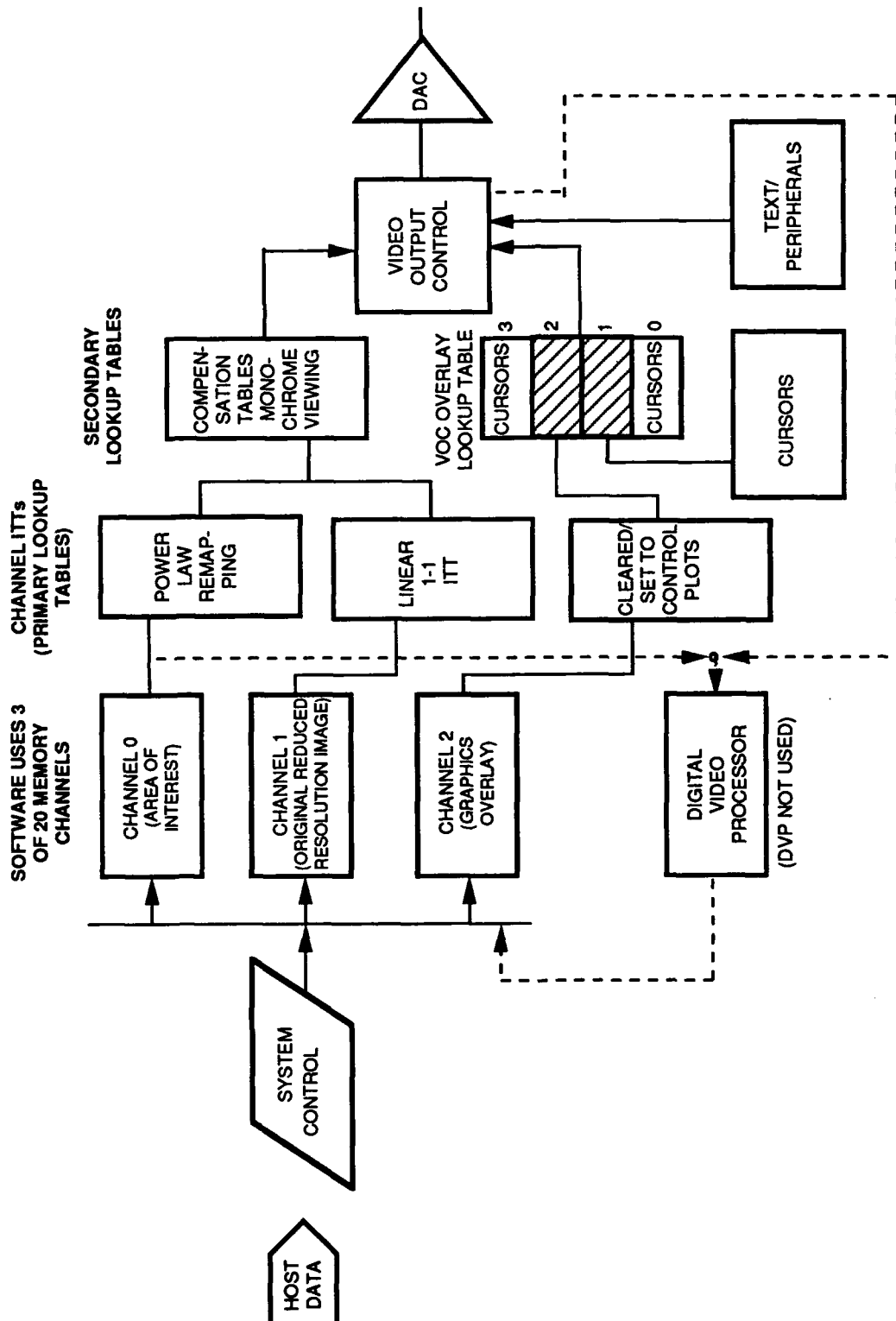
Figure 10: Hardware Structure Related to Processing Function and Data Flow

- A is the amplitude data value

- AO is the minimum amplitude

- ASAT is the amplitude saturation value for the remapping

- P is the power law exponent

The following equations will set forth a relationship between the power law exponent, P, and the mean density of the film, <D> (Equation 15). Density is defined here as the optical density (or absorbancy), which is the logarithm of the reciprocal of the transmittance. Furthermore, input to the film recorder is proportional to the density of the exposed film (Equation 16). Equation 17A expresses the film recorder input count in terms of the power law exponent, and in terms of film density. The resultant remapping function relates amplitude data to film recorder input counts (Equation 18). Equation 18 is the first remapping function. Replacing Equation 19 for Equation 15 gives the second remapping function (Equation 20). Looking again at the previously defined equations:

$$T = TMIN \qquad\qquad for \quad A \le A0 \qquad\qquad (9A)$$

$$T = TMAX \left(A/ASAT\right)^P \qquad for \quad A0 \le A \le ASAT \qquad (9B)$$

$$T = TMAX \qquad\qquad for \quad ASAT < A \qquad\qquad (9C)$$

Taking the logarithm of the transmittance:

$$\log T = \log TMAX + P \log (A/ASAT) \quad for \quad A0 \le A \le ASAT \qquad (10)$$

By definition:

$$D = - \log T \qquad\qquad\qquad (11A)$$

Where:

$$DMIN = - \log TMAX \qquad\qquad (11B)$$

$$DMAX = - \log TMIN \qquad\qquad (11C)$$

Combining equations 10 and 11A, and solving for D:

$$D = -\log TMAX - P (\log (A/ASAT)) \qquad (12A)$$

Substituting 11B and rearranging:

$$D = DMIN + P (\log ASAT - \log A) \qquad (12B)$$

The saturation amplitude, ASAT, should be a multiple of the mean, median, or mode of the amplitude histogram (AM), since the ratio of ASAT to any of these statistical functions is found to be fairly stable in images of natural scenes. Adding and subtracting log AM to the right side of Equation 12B gives:

$$D = DMIN + P (\log (ASAT/AM) + \log AM - \log A) \qquad (13)$$

23

DMIN, P, and ASAT/AM are constants, so that the mean film density <D> is:

$$<D> = DMIN + P (log (ASAT/AM) + log AM - <log A>) \qquad (14)$$

Solving for P gives the power law exponent as a function of scene density:

$$P = \frac{<D> - DMIN}{log (ASAT/AM) + log AM - <log A>} \qquad (15)$$

For a hardcopy film recorder the output density, D, is proportional to the recorder input count, C:

$$D = DMAX - ((C/255) (DMAX - DMIN)) \qquad (16)$$

Using Equation 16, if the input count C equals 0, then D = DMAX, and the transmittance (analogous to display intensity) is at a minimum. Likewise, if the input count C equals 255, then D = DMIN, and the transmittance is at a maximum.

Expressing the recorder input count as a function of P, by substituting Equation 12B into 16:

$$C/255 = \frac{DMAX - DMIN + P (log ASAT - log A)}{DMAX - DMIN} \qquad (17A)$$

Substituting for DMIN and rearranging:

$$C/255 = 1 - P \left(\frac{log ASAT - log A}{DMAX - DMIN} \right) \qquad (17B)$$

Adding and subtracting log AM to the right-hand side of Equation 17B:

$$C/255 = 1 - P \left[\frac{log (ASAT/AM) + log AM - log A}{DMAX - DMIN} \right] \qquad (17C)$$

Substituting the value of P (Equation 15) into 17C and letting AR be the ratio, ASAT/AM:

$$C/255 = 1 - \left(\frac{<D> - DMIN}{DMAX - DMIN} \right) \left(\frac{log AR + log AM - log A}{log AR + log AM - <log A>} \right) \qquad (18)$$

Equation 18 expresses the first of the two remapping functions that transform the 11-bit amplitude data, A, to the 8-bit remapped data. In this remapping, the power law is calculated based on the average logarithm of A, <log A> to give a true average density <D> of the remapped image.

The second of the two remapping functions associates a particular density value with the ASAT ratio. The power law exponent in this set of remappings is calculated by using the logarithm of the AM value (mean, median, or mode of the

24

amplitude histogram) instead of the average logarithm of A, and using the corresponding density value in place of the average density.

Letting:

$$\log AM = <\log A>$$

and

$$<D> = D(AM)$$

Equation 15 becomes:

$$P = \frac{D(AM) - DMIN}{\log (ASAT/AM)} \qquad (19)$$

Where D(AM) is the density value of AM.

Substituting Equation 19 into 17C, and letting AR = ASAT/AM:

$$C/255 = 1 - \left[\frac{D(AM) - DMIN}{DMAX - DMIN}\right]\left[\frac{\log AR + \log AM - \log A}{\log (ASAT/AM)}\right] \qquad (20)$$

This is the second remapping function.

ASAT/AM and <D> or D(AM) (depending on which set of remapping functions is being described) are input by the user via joystick or trackball. ASAT/AM values are limited to values ranging from 1 to 1000, while <D> values are scaled density values ranging from DMAX to DMIN. The ASAT ratio and the <D> value dynamically control the remapping of the image. As the user modifies the values, the remapping Intensity Transformation Table (ITT) is updated.

Image dependent variables that are calculated from the normalized amplitude histogram are: log AM and <log A>. Respectively, these are the logarithm of the mean, median or mode of the decompressed amplitude data, and the average logarithm of the amplitude data.

System constants include CMAX, DMIN, and DMAX, where CMAX is the maximum input count to the film recorder, and DMIN and DMAX are minimum and maximum allowable film densities.

In conclusion, the remapping functions are calculated interactively and the DeAnza ITT (Intensity Transformation Table, or Primary Look-Up Table) stores the film recorder input associated with the original amplitude data.

Relating Film Recorder Inputs to Display Inputs

Film recorder inputs are related to the CRT input counts in the following manner. Look-Up Table data for display linearization was calculated based on measured brightness (i.e., where brightness is directly related to the eye's response) vs. digital CRT input. Assuming this is true:

$$B = BMAX \ (J/JMAX) \quad \text{for} \quad 0 < J \leq 255 \tag{21}$$

where J is the digital input used to drive the CRT display.

Repeating equation 16 which relates film density to the input film recorder:

$$D = DMAX - (DMAX - DMIN)(C/CMAX) \tag{22}$$

Since display brightness is analogous to film transmittance:

$$D = - \log \ (B/BMAX) \tag{23}$$

Combining Equations 21, 22, 23:

$$DMAX - (DMAX - DMIN)(C/MAX) = - \log \ (J/JMAX) \tag{24}$$

Solving for J/JMAX:

$$J/JMAX = 10^{-DMAX} 10^{(DMAX-DMIN)(C/CMAX)} \tag{25}$$

Applying Equation 21 to Equation 23, the film recorder inputs, J, are related to the display inputs, C, by:

$$J/JMAX = \left(\frac{BMIN}{BMAX}\right)\left(\frac{BMAX}{BMIN}\right)^{C/CMAX} \tag{26}$$

where BMAX and BMIN are the maximum and minimum displayable brightnesses.

Therefore, film recorder input can be directly related to desired display brightness by a single look-up table.

Software Capabilities

The program reads an image from disk or from magnetic tape and loads the image into Channel 0 of the image processor. The program is menu-driven and leads the operator through the various options. For each image displayed histograms can be calculated, plotted and remappings can be performed on operator-selected regions within an image. The image can be remapped as many times as desired, and remapped histograms and look-up tables can be saved on disk.

Program Capabilities include:

- Selection of regions of interest within the image
- Count-Normalized histogram calculation of selected regions
- Writing histogram data to a file and/or overlaying a plot of the histogram upon the image
- Calculation of various statistics from the generated histogram: these include Average, Average Logarithm, Median, and Mode Value of the image data

26

- Selection of any one of six sets of remapping parameters
- The ability to vary selected default parameters that control the remapping
- Save the remapped image histogram and/or look-up tables

Operation of the Remap Software

The section describes the operation of the software in terms of program initialization and of the menu-driven remapping operations.

Initialization:

Upon entry to the remap program, the user is prompted via the terminal for the DeAnza logical unit number and for the name of the file containing the compensation table to be loaded into the Secondary Look-Up Table (LUT) sections. The following is an example of the initialization prompts and a sample set of operator responses. The ">" sy ^hol is a system-level prompt telling the operator to input information. The operator responses are shown on the same line and immediately after the prompt.

```
Enter Logical Unit Number
> 0
Enter Filename For LUT
> Linear.LUT
```

The program next checks the switch settings on the joystick or trackball control and informs the user if any switches are not set correctly. The user must change the switch settings before the program will continue.

Next the user is prompted for the source of input (tape or disk) and for the image file name:

```
Select Source of Input
1 - Tape
2 - Disk
Enter number corresponding to source
> 2
Enter disk filename
> (DIR)NEWIMAGE.DAT
```

If the file exists, the image will be loaded and the terminal displays a "WORKIING" message. If the file is not found, a "File Not Found" message is displayed and the program prompts for a valid file name.

The above initialization steps are executed upon entry to the remap program and each time the user requests a new image (Selection 7, Menu 4).

A reduced resolution image (512 x 512 pixels) of a large format image (either 1024 x 1024 or 2048 x 2048 pixels) is loaded in Channel 1 and displayed. A rectangle or "corral" representing the size of a true 512 x 512 pixel subregion of the reduced resolution image is displayed in the center of the image. The operator

27

is instructed to "Use the joystick to move the corral" and "Press ENTER button on joystick when positioned over the desired area". After the user responds, that area of the image is written to memory Channel 0 with the original resolution restored. The entire original reduced resolution image is saved in memory Channel 1 so operations can be performed on other desired areas without reloading the image.

Next the selected area of interest is displayed. On the upper left-hand corner of the display, the user is prompted to select a region of interest . (SELROI):

```
Select Area of Interest
------------------------
1) Select Upper Left Corner
2) Select Lower Left Corner
3) Done
```

The joystick or trackball is used to position the cursor on the far left of the selection line. The selection at which the cursor is positioned is displayed in reverse video mode so that it is easily discernable. When the cursor is positioned at the desired selection, the user must depress 'ENTER' for the desired function to be performed. This is the way in which all menu selections are made. (MENU, READJOY)

In the selection of an area of interest, if "DONE" is selected before a corner is set, the entire displayed area is the region of interest. When selecting a corner, the user moves the joystick or trackball and a rectangular box is drawn to show the region included in the selection.

After the region of interest is selected, the program calculates the normalized histogram of the region and several statistics based on this histogram.

The selection of a region of interest and the histogram and statistical calculations are performed upon entry to the program each time the user requests an image (Selection 7, Menu 4), and each time the user requests remapping of an existing image (Selection 6, Menu 4).

Menu Description

After initialization, the remapping software is driven by four menus: a main menu, two menus to select remapping parameters, and a menu to utilize remapped data. Their formats are described in the rest of this section.

MENU 1:

Menu 1 is displayed after an image has been loaded, a region of interest has been selected, the histogram for that region has been calculated, and mean, median and mode information has been calculated.

```
PLEASE MAKE SELECTION
---------------------
1. WRITE HISTOGRAM TO A FILE
2. PLOT THE HISTOGRAM
3. REMAP THE IMAGE
4. SET THE DISPLAYED DENSITY RANGE
```

5. QUIT

The user positions the cursor as described in the initialization, and presses 'ENTER'. Each of these possible selections will be discussed in turn.

Selection 1 writes the histogram, normalized by the number of pixels in the selected region of interest, to a file. The user is prompted by the terminal to input a file name.

Selection 2 plots the histogram in the upper left-hand corner of the monitor, overlaying the image. The user must depress 'ENTER' on the joystick/trackball to return to Menu 1.

Selection 3 controls remapping of the image. The remapping options consist of: (1) selecting a remapping function, (2) selecting individual parameter values with which to generate new remapping, and (3) routing of the remapped data. Control is transferred to Menus 2, 3 and 4 respectively.

Selection 4 sets the displayed density range of the image so that amplitude counts are linearly distributed over a selected range of density values.

The image is displayed with the cursor position in the center of the x-axis. The y-axis coordinate is controlled by the joystick/trackball displacement. At the bottom of the display, the maximum displayable density (density range) and minimum digital input count into the display (CO) are shown:

```
_____
   Density Range = .73, CO = 146
_____
```

By moving the joystick, the y position will change the density range and the associated CO value. The secondary LUT will be updated so the image can be viewed as the density range is changed.

Selection 5 exits to the operating system.

MENU 2

Menu 2 prompts the user for selection of a remap function and calls Menu 3 to interactively input parameters to control the remapping. There are six sets of statistics that define the remapping function (MODE2). The operator is prompted to select one:

```
PLEASE MAKE SELECTION
_____
1. ASAT/AMED  VS. DAVE
2. ASAT/AMODE VS. DAVE
3. ASAT/AAVE  VS. DAVE
4. ASAT/AMED  VS D(AMED)
5. ASAT/AMODE VS. D(AMODE)
6. ASAT/AAVE  VS. D(AAVE)
```

The above six sets of statistics are used in selecting the saturation amplitude (ASAT) and the power law remapping (P). The ASAT ratio is used to select the

saturation value in the amplitude histogram, and the density ratio controls the selection of the power law.

Variable definitions are:

- ASAT   SATURATION AMPLITUDE
- AMED   MEDIAN OF THE AMPLITUDE HISTOGRAM
- AMODE   MODE OF THE AMPLITUDE HISTOGRAM
- AAVE   AVERAGE VALUE OF THE AMPLITUDE HISTOGRAM
- DAVE   AVERAGE DENSITY OF THE REMAPPED IMAGE
- D(AMED)   AVERAGE DENSITY CORRESPONDING TO MEDIAN AMPLITUDE AFTER REMAPPING
- D(AMODE)   AVERAGE DENSITY CORRESPONDING TO MODE AMPLITUDE AFTER REMAPPING
- D(AAVE)   AVERAGE DENSITY CORRESPONDING TO AVERAGE AMPLITUDE AFTER REMAPPING

Setting the saturation value of the remapped image is comparable to changing the contrast of the image. Since transmittance in a duplicate positive and display brightness on CRT are analogous, changing the density parameter is equivalent to changing the display brightness.

In selecting an ASAT ratio, the operator is choosing a method of defining the saturation value: as a multiple of the median of the amplitude histogram, as a multiple of the mode of the amplitude histogram, or as a multiple of the average of the amplitude histogram.

In selecting the density parameter, the operator is selecting the way in which the power law exponent is calculated. In the first three selections, DAVE is the average density after the remapping. This means that the power law exponent is calculated to give an average density that equals the value that the user inputs. For selections 4 through 6, the power law is calculated based on the density value that corresponds to either the median value of the amplitude histogram, the mode of the amplitude histogram, or the mean of the amplitude histogram.

The user positions the cursor at the beginning of each selection through joystick control, and presses 'ENTER' when the selection is complete.

After selecting a remap function, Menu 3 provides the option to control ASAT and P for the remapping.

MENU 3

Through Menu 3, the user can change ASAT values (x-axis) and/or the density values (y-axis), and interactively view the image on the CRT as the remapping occurs.

```
PLEASE MAKE SELECTION
_____
1.    UNLOCK BOTH VALUES
2.    LOCK X-AXIS
3.    LOCK Y-AXIS
4.    REMAP COMPLETE
```

By unlocking both values, both the saturation amplitude and the density of the remapped image can be changed. By locking the x-axis, only the density value can be changed. Conversely, locking the y-axis allows only the saturation value to be changed.

The operator makes a selection and depresses 'ENTER'. After 'ENTER' is depressed, a cross-hair is displayed at the center of the image. By using the joystick, x and y values are changed and displayed at the bottom of the monitor. At the same time the image is remapped by modifying the Image Transformation Table for that channel.

X and y values are displayed as follows:

```
_____
    ASAT/AAVE = 50        DAVE = .4
_____
```

The operator continues to modify the parameters until the interpretability of the image is judged to be optimum.

If, for example, the above value of ASAT/AAVE was selected for the final remapping, the saturation amplitude for the remapped image would be 50 times the average value of the amplitude histogram.

If the average density after remapping (DAVE) is set to a value of .4, and if the display brightness that corresponds to the maximum transmittance, BMAX, equals 255, then the brightness associated with the average density will be 102 since:

$$D = - \log (T)$$

$$= - \log (B/BMAX)$$

$$= \log (BMAX/B)$$

So:

$$10^D = BMAX/B$$

And:

$$B = BMAX/(10^D)$$

$$= 255/10^{0.4}$$

$$= 101.52$$

31

When the image is displayed in the most interpretable form, the operator selects 'REMAP COMPLETE' and the normalized histogram and histogram statistics are calculated. Control then transfers to Menu 4.

MENU 4

Menu 4 gives further remapping functions:

```
PLEASE MAKE A SELECTION
------------------------
1.   WRITE HISTOGRAM TO FILE
2.   PLOT THE HISTOGRAM
3.   WRITE THE LUT TO A FILE
4.   PLOT THE LUT
5.   SET THE DISPLAYED DENSITY RANGE
6.   REMAP THE SAME IMAGE AGAIN
7.   START OVER WITH A NEW IMAGE
8.   QUIT
```

Selection 1 writes the remapped histogram to a file and Selection 2 plots the remapped histogram onto the upper middle portion of the display, as in Menu 1.

Selection 3 writes the Look-Up Table to a file, while Selection 4 plots the LUT in the upper right portion of the display.

With Selection 5 the operator sets a displayed density range, as in Menu 1.

Selection 6 remaps the same image again: the user selects a new area of interest, a detailed region of interest, and returns to Menu 1.

In Selection 7, the program returns to the initialization, prompts for source of input (tape or disk), and repeats the entire process.

Selection 8 exits the program and returns control to the operating system.

Software Structure

This section will first correlate software functions with the DeAnza IP8500 architecture. Second, block diagrams of the software hierarchy will be presented, along with a brief description of the remapping subroutines.

Software Related to DeAnza Architecture

The DeAnza IP8500 features used by the software are:

- Three of the twenty available 512 x 512 x 8 bit memory channels. Two are used for imagery, and one for graphics.

- Intensity Transformation Tables (ITT) for each memory channel used.

- Video Output Controller (VOC)

- VOC secondary Look-Up Table (LUT) or "secondary" LUT

- VOC "overlay": Look-Up Table

- Joystick and Trackball Input Devices
- Alphanumeric generator
- Cursor unit

The following points relate the software to Figure 10:

(1) The reduced resolution log-compressed data, Y, is read from disk or tape to Channel 1

(2) Channel 1 ITT is loaded with a linear Look-Up Table (LUT), where input equals output, at the start of the program, so that the original image is displayed in a known display brightness representation at the start of the program.

(3) After the user selects an area of interest by moving the "corral" over the desired area, ITT selection 0 of Channel 0 is loaded with a linear LUT and the area is read from disk and written to Channel 0 with the initial resolution restored.

(4) Next, a region of interest (within the previously selected area) is chosen by the user.

(5) The histogram calculation is performed by reading pixel values from the selected regions within Channel 0, and uses an array to sum the number of times a pixel value occurs. For remapped images, the pixel value is used as an index into the ITT where the remapped intensity is stored. Histograms are normalized by the total number of pixels in the considered region. Histogram data is stored in REMAP.INC include file.

(6) Histogram mean, median and mode calculations are straight forward. A delogging function, DELOG, is used to decompress the log-compressed data, Y:

$$A = DELOG\ (Y) = (2047)(2)^{[(Y-255)/16]}$$

Software Hierarchy and Subroutine Descriptions

Figure 11 is a functional block diagram of the top level of the remapping software. Functions are performed from left to right. Figures 12, 13 and 14 are functional block diagrams of the various menu options available. Subroutines that perform each function are shown beneath the appropriate function block.

The following is a list of remapping subroutines with a brief description of each routine:

CALSTATS	Calculate mean, median, mode statistics from histogram
CHECK	Check switch settings on joystick or trackball control
CORRAL_CTL	Controls corral movement, where corral represents a 512 x 512 area over a reduced resolution image

Figure 11: Functional Block Diagram Of Remapping Software, Level 1, With Two Levels Of Major Subroutine Calls
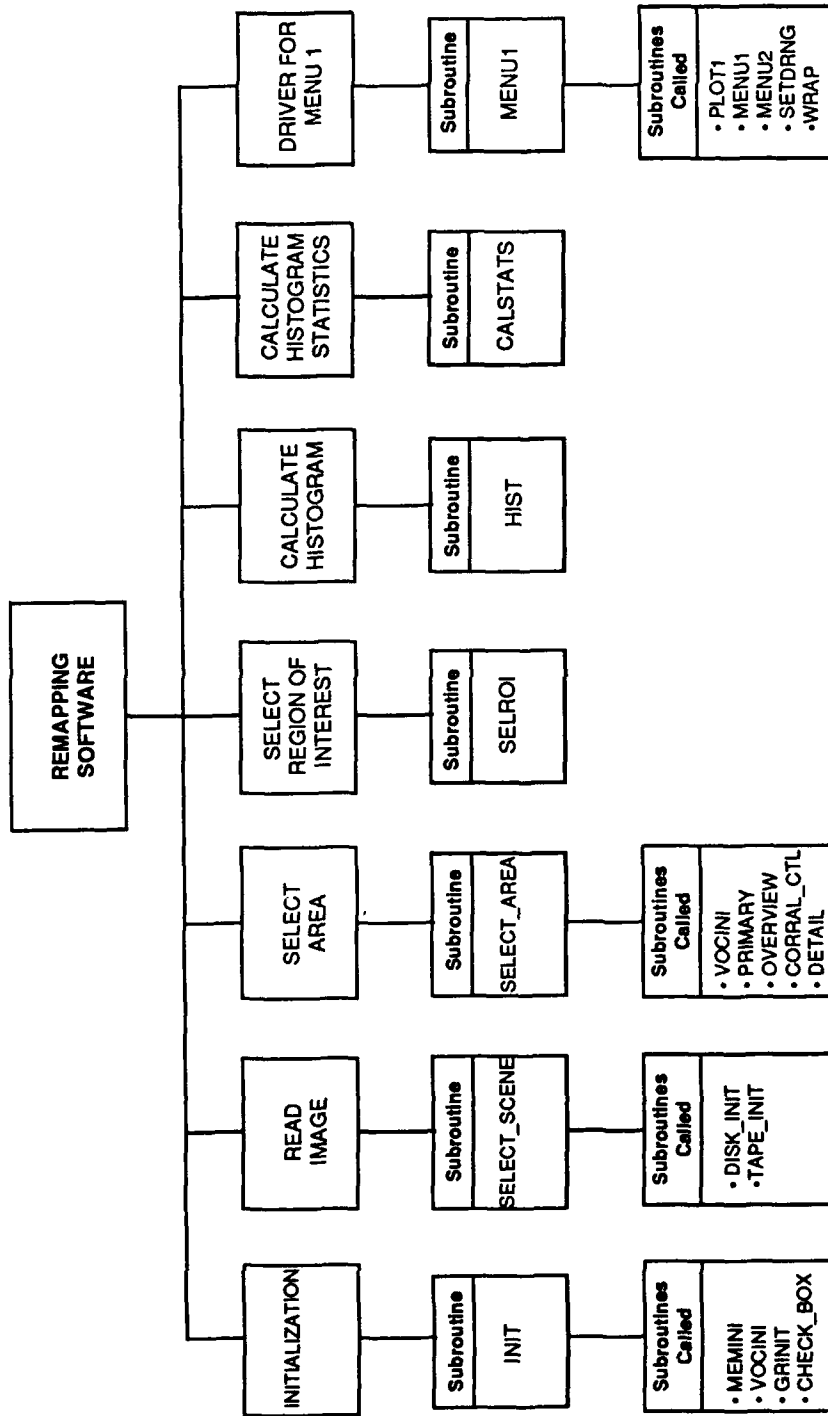
[Note: Subroutines Called From Left To Right]

34
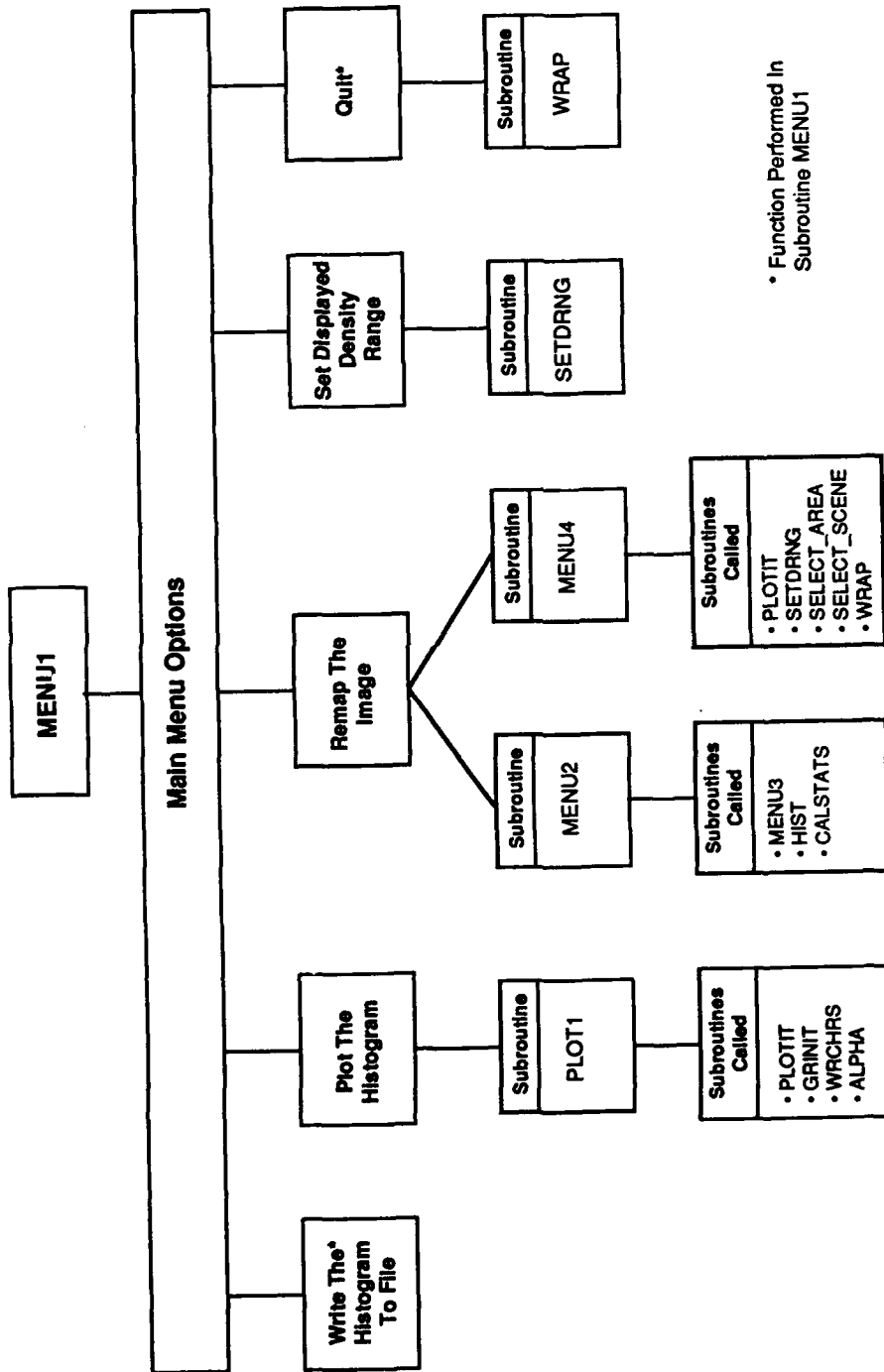
Figure 12: Functional Block Diagram of Subroutine MENU1,
With Two Levels Of Major Subroutine Calls

MENU2

SELECT REMAPPING FUNCTION AND
INTERACTIVELY CONTROL REMAPPING

SELECT*
REMAPPING

INPUT REMAPPING
PARAMETERS AND
VIEW REMAPPED
IMAGE

Subroutine

MENU3

Subroutines
Called

• REMAPFN
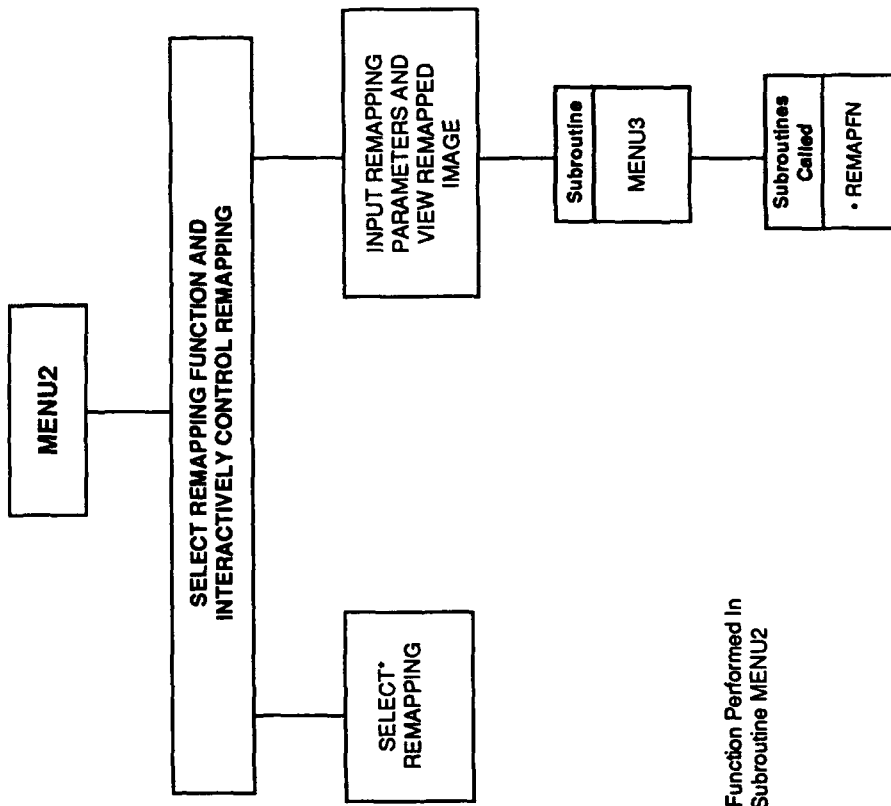
• Function Performed In
Subroutine MENU2

Figure 13: Functional Block Diagram of Subroutine MENU2,
With Two Levels Of Major Subroutine Calls
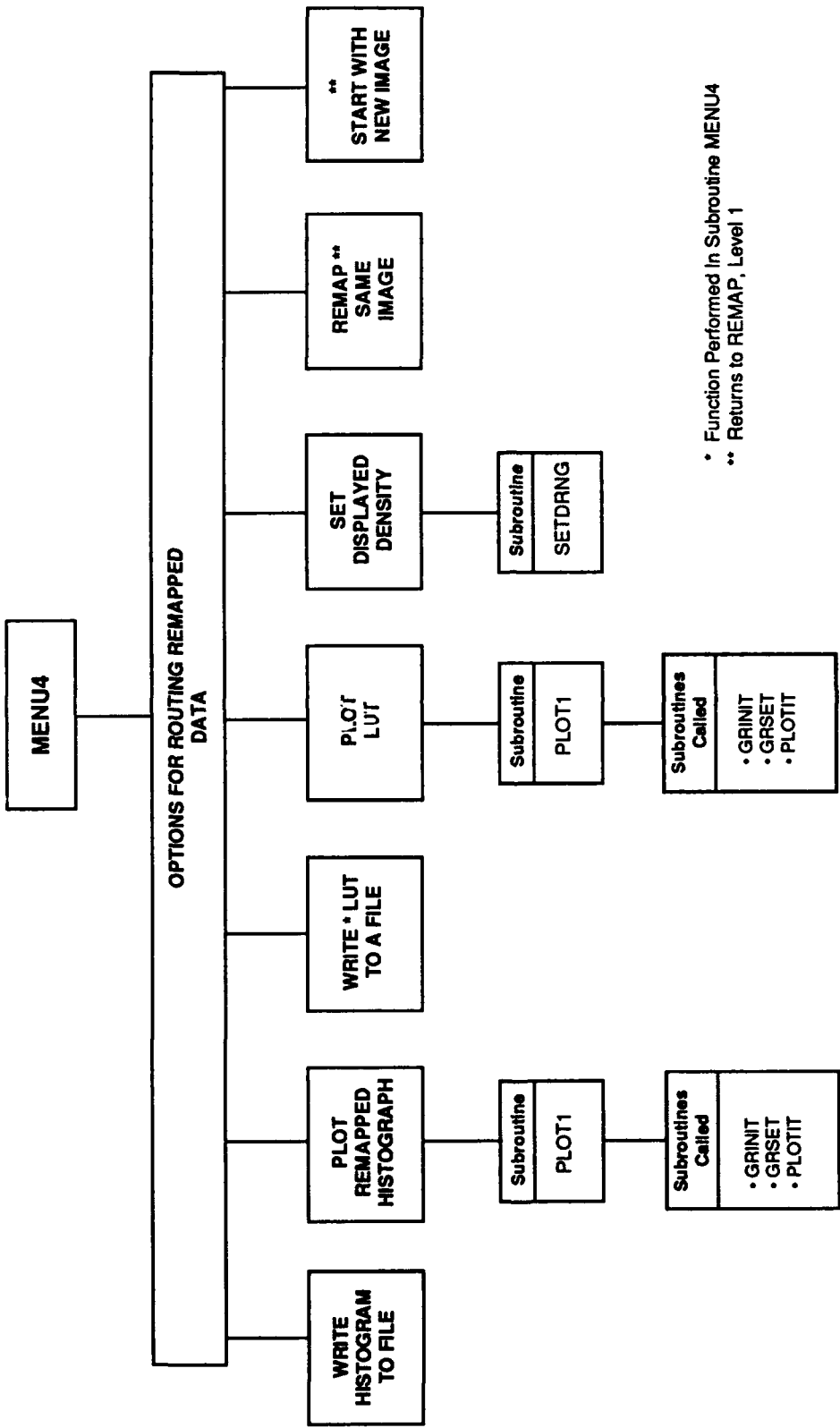
**Figure 14: Functional Block Diagram of Subroutine MENU4, With Two Levels Of Major Subroutine Calls**

CURSOR_INIT	Initialize programmable cursor
DETAIL	Reads 512 x 512 pixels from base memory and writes to Channel 0
DISK_INIT	Reads image file and writes out 2048 x 2048 base memory file
DISK_READ	Read one record from disk
DISK_WRITE	Write one record to disk
DSPMENU	Display menu options and get operator response
GRSET	Display menu options and get operator response
GRINIT	Initialize graphics channel
HIST	Calculate count-normalized histogram
INIT	Initialize DeAnza -- Calls MEMINI, VOCINI, GRINIT
LDGRLUT	Load Graphics Look-Up Table
LIMIT_COR	Keep corral within bounds of DeAnza screen
MEMINI	Initialize memory planes and channels
MENU1	Driver for Menu 1: Writes histogram to file, plots histogram, remaps image, sets displayed density range
MENU2	Driver for Menu 2: Selects remap function, changes saturation amplitude and density parameters to interactively remap image, calculates histogram and histogram statistics
MENU3	Called by Menu 2: Allows operator to change remappingparameters and interactively remap image until image is displayed at maximum interpretability
MENU4	Driver for Menu 4 - Remapped data menu: Writes remapped histogram to a file, plots remapped histogram, writes remapping look-up table to a file, plots look-up table, sets displayed density range, remaps same image again or starts with a new image
NEWSTUFF.INC	Include file with general information needed by all subroutines
OVERVIEW	Writes a reduced resolution of 2048 byte image to Channel 1
PLOT1	Driver for plot routines
PLOTIT	Plots data, scales data, labels plot, and tics and labels axes
PLOTDAT	Block data with plot parameters
PRIMARY	Writes a reduced resolution of a 1024 record by 2048 byte image to Channel 0

REMAP	Main driver
REMAP.INC	Include file that contains commons with remap data
REMAPFN	Performs remapping functions
SELECT_AREA	Has operator select a 512 x 512 area of base memory and writes this area (with restored resolution) to Channel 0. Calls OVERVIEW or PRIMARY or DETAIL
SELECT_SCENE	Driver for tape or disk input of original image. Calls TAPE_INIT or DISK_INIT
SELROI	Selects a region of interest from which histogram calculation and remapping will be performed
SETDRNG	Sets displayed density range so amplitude counts are linearly distributed over a specified range of density values
TAPE_INIT	Reads data from tape and writes to disk
TAPEREAD	Reads from tape
TAPE_REWIND	Rewinds tape
TAPESKIP	Skips files on tape
WRCHARS	Writes segmented characters to graphics channel
WRAP	Exits to operating system
XIP8JOY	Reads status data from the joystick or trackball interface unit

V. IMAGE QUALITY MEASUREMENT TECHNIQUE EVALUATION

Background

Automated algorithms have been evaluated and used at SAIC in testing SAR image quality in terms of IPR width and peak sidelobe ratio. The algorithms are currently hosted on a VAX-11/750 and measure imagery as displayed on an I^2S workstation.

SAIC analyzed and evaluated algorithm performance as a function of shift between the sampling train and the point target image, in the presence of various amounts of phase error and also for various SAR aperture weightings. SAIC also performed extensive statistical evaluation of a modified Gaussian interpolator to fit the point target response and measure -3 dB and -15 dB IPR.

Based on the results of this work the following algorithms were selected to be used on a regular basis to evaluate SAR image quality:

- To measure -3 dB IPR width, an algorithm developed for a classified program by another contractor was chosen. This involves upsampling/interpolation via Fourier transformation.

- To measure -15 dB IPR width, a modified Gaussian interpolator is used. This consists of a true Gaussian profile connecting on both sides to straight line segments, and slopes matched to the Gaussian at the point of connection.

- To find sidelobe peaks in the range/cross-range plane, another contractor's search algorithm is available. This obtains sidelobe maxima as a function of radial distance from the IPR peak. As a practical matter the peak sidelobe is measured at SAIC in axial IPR cuts, displayed in range and cross-range for each pixel. This approach not only locates, with very high probability, the largest sidelobe, but also provides insight into the sidelobe structure, thus aiding in system trouble shooting.

- To measure contrast ratio, if the imaged scene contains no-return areas or radar shadows surrounded by uniform terrain and if it contains at least one target of known cross-section (a corner reflector), a less automated measurement is used. It involves operator designation of the boundaries of the areas considered as no-return and as adjacent uniform terrain, respectively. Mean and standard deviation of the pixel intensities are computed for both the terrain and the no-return areas, in order to measure a first-order departure from Rayleigh statistics and thereby provide an indirect check on the uniformities.

Functional Description of the Algorithms

Impulse Response -3 dB Width Measurement

Summary: FFT interpolation is used to upsample the imagery by a factor of eight. The peak and -3 dB widths are determined using the upsampled imagery.

Input Data Format

The data are assumed to be stored in a compressed form with input image levels $P(I,J)$ related to amplitude $A(I,J)$ levels by:

$$A(I,J) = \exp(k \times (P(K,J)) - 255)$$

where
$$K = .03611898 \quad \text{(a scaling constant)}$$

$$P(I,J) = \text{an 8-bit pixel}$$

$$A(I,J) = \text{a real floating point amplitude value}$$

The data are converted from $P(I,J)$ to $A(I,J)$ before processing.

Sub-Image Extraction

Given the location of the peak pixel within the image, (I_0, J_0), an 8 x 8 pixel sub-image is removed and placed in an array $D(I,J)$. The alignment used is $D(4,4) = A(I_0, J_0)$. The inverse log compression described above is performed to obtain amplitude data.

Two-Dimensional FFT

The two-dimensional Fourier transform of the subset is computed and the result padded to a size of 64 x 64 to achieve upsampling.

Inverse FFT

The inverse two-dimensional FFT of the padded data is computed, resulting in a 64 x 64 upsampled version of the image. The peak of the upsampled data is located and its location converted to original (without upsampling) pixels.

Calculation of -3 dB Width

Using the upsampled data, the samples which straddle the -3 dB level (.7071 x peak) are determined in the range and azimuth direction. Linear interpolation is used to find the -3 dB widths in the range and azimuth directions. The -3 dB widths in pixels are multiplied by constant factors to convert pixel spacings to feet.

Impulse Response -15 dB Width Measurement

The FORTRAN program MAXSLICE is used to compute the -15 dB width of an impulse response function. The sampled data values are chosen by taking a row or column slice through a two-dimensional array of image pixels.

41

The algorithm works as follows: The set of data points is raised to the 0.3 power. To this new set of points, a Gaussian interpolator applies an upsampling of x 8. The interpolator works by convolving a modified Gaussian pulse with the delta functions scaled by the data points.

The modified Gaussian pulse has a width controlled by the parameter sigma, which is set for these measurements to be 60% of the sample interval. At a given breakpoint the Gaussian tail is dropped in favor of a straight line segment which falls off to zero. At this breakpoint, the modified Gaussian function and its first derivative are continuous. To interpolate, at seven intermediate positions between two of the data points, the contributions from the nearest five Gaussian pulses, weighted by the amplitude of the data samples, are summed. Thus, an upsampling by 8 is produced, and these samples are then raised to the 3.3333 power to return them to the original input space.

To measure the width of the impulse response, the peak and the two -15 dB levels are found by applying linear interpolation to the upsampled data set. The distance between the two -15 dB points is the width of the IPR in pixels.

Peak Sidelobe Measurements

The FORTRAN program MAXSLICE is used to compute the peak sidelobe level of an impulse response function. The sampled data values are chosen by taking a horizontal or vertical slice through a two-dimensional array of image pixels. Except for squint operation of the radar, these directions correspond to the two sidelobe axes.

The original set of samples from the slice, without upsampling and interpolation, is inspected by a peak detection circuit. Any point both neighbors of which are lower in amplitude, is considered a peak and is copied into a table. When the entire set of samples has been tested, the table is translated into decibels, and the maximum value read out as the peak sidelobe level.

In squint operation, MAXSLICE may miss the nonorthogonal cross-range sidelobes. For squint images, program SLICE is used. Program SLICE works by defining a line that passes through the peak pixel and a point selected by the user with the trackball along the sidelobe structure. The sample values examined by the program are those pixels which define the shortest distance in total adjacent pixels along a straight line extension of the segment defined by the designated points.

Accuracy of the IPR Evaluation

The pulsed/sampled SAR signal becomes a sampled/quantized version of the point target image (impulse response) at the output of the SAR processor. Ideally, the -3 dB width and the -15 dB width of the IPR would be attributes of the continuous output. On a continuous output they could be obtained (at least in principle) exactly. On the sampled/quantized output, the measurement must be approximate, due to limitations in the reconstruction of a continuous signal from its processed samples.

42

Accuracy of the -3 dB Width Measurement

SAIC has sampled and quantized the continuous point target response according to the parameters of a developmental SAR system, processed the samples using the -3 dB width measurement algorithm and obtained a comparison between the measurement output and the true IPR. This was performed for two system modes (listed in the order of increasingly finer resolution), for three SAR aperture and range pulse weightings, and for various amounts of quadratic phase error. The comparison was obtained as a function of the shift of the sample train with respect to the peak of the continuous point target response.

The error depends on the amount of the shift between the peak of the continuous point target response and the sample train. For any given sample train shift, there would be a small spread of the error values as a function of peak target amplitude, due to the 8-bit quantization of the output. This variable was not considered in the runs, since its impact is less than 0.5Δ rms, and the bias it introduces is negligible.

Since the sample train shift, as a random variable, can be considered to be uniformly distributed, the measurement error averaged over the sample shift can be considered to be the measurement's bias error. This bias error has been tabulated in Table II for Mode A, and in Table III for the finer resolution Mode B.

Table II

-3 dB Width Measurement Bias (Per Cent)

Mode A

SAR Aperture Weighting \ Quadratic Phase Error	0	30	60	90	120	150	180
Uniform	-1.7	-1.5	-1.0	1.9	9.0	-0.4	-9.1
Cosine	0.9	0.1	1.3	3.9	7.7	0.2	-0.6
-35 dB Taylor	0.6	-0.5	-0.7	-0.3	0.2	0.1	-1.4

Table III

-3 dB Width Measurement Bias (Per Cent)

Mode B

SAR Aperture Weighting	Quadratic Phase Error 0	30	60	90	120	150	180
Uniform	-4.0	-3.5	-2.6	0.7	8.2	-1.2	-3.6
Cosine	-0.4	-0.5	0.4	3.3	7.5	0.0	-0.3
-35 dB Taylor	0.4	-0.1	-0.4	0.0	0.6	0.9	-2.3

The values of the true -3 dB widths were determined by a computerized FFT routine at SAIC. The appropriate weighting function is first generated, along with the specified amount of quadratic phase error. The weighting is sampled at 64 points, and an equal amount of zero-fill added, padding the arrays out to 128 points. The complex FFT is taken, generating 128 frequency-domain samples at twice the Nyquist rate. A four-point LaGrange interpolation is performed on the magnitude to generate seven intermediate samples for each of the original data points, for 1024 total points. The interpolation is done so that the new points are computed for the impulse response segment lying between the middle two of each group of four points used in the process, the region where the LaGrange fit is most accurate. A linear interpolation is then used in computing the -3 dB width of the IPR.

This method of computing the "true" width, that is the -3 dB width of the continuous point target response, was spot checked for a case of extreme quadratic phase error. The check was made for uniform weighting and 180 degree quadratic phase error, and it was performed in the "reverse direction". The SAIC algorithm indicated a -3 dB width of 2.6335 for the continuous point target response (as compared to 0.8859 for the case with no phase errors). The actual Fourier integral was calculated at the half-width 2.6335/2, and the level of the response was found to be -3.0066 dB below the peak, instead of exactly -3.0000 dB, representing an error of about 0.08%.

44

Accuracy of the -15 dB Width Measurement

IPR width at the -15 dB level is measured using the modified Gaussian interpolator:

$$g(X) = \begin{cases} e^{-\dfrac{X^2}{2\sigma_g^2}} & ;|X| \le X_0 \\[2em] e^{-\dfrac{X^2}{2\sigma_g^2}}\left[1 - \left(\dfrac{2 - |X|}{2 - X_0}\right)\right] & ;X_0 \le |X| \le 2 \end{cases}$$

where:

$$X_0 = 1 + \sqrt{1 - \sigma_g^2}$$

and:

$$\sigma_g = 0.60$$

with X normalized to the sampling interval. It is seen that g(X) is a true Gaussian profile for $X \le X_0$ and is then connected to the point (2,0) with a line segment in such a way as to maintain continuity of g(X) and its first derivative on the interval (-2,2).

To evaluate the performance of the measuring algorithm at the -15 dB level, Monte Carlo runs were made to allow for occasional occurrences of large phase and amplitude errors across the SAR aperture, for which the first sidelobes may reach or exceed the -15 dB level, merging into the main lobe of the IPR. For a realistic phase and amplitude, errors were represented. Their modeled standard deviations and statistical distributions are given in Table IV, as conservatively representative of recent system design.

Monte Carlo runs were made with no system errors (only randomized sampling shift), with system errors as characterized in Table II, and also with system errors that had twice the standard deviations of a system clearly not within specifications. The results of the Monte Carlo runs are given in Table V for cosine and -35 dB Taylor weightings. Uniform weighting was not considered for this measurement, since for such weighting the no-error first sidelobe itself exceeds the measurement level of -15 dB; thus, even for small system errors, it merges with the main lobe.

45

Table IV
Phase and Amplitude Error Entries
In The Monte Carlo Runs

Normalized Amplitude Errors Total Excursion	Standard Deviation	Distribution
Linear	.135	Zero Mean Gaussian
Quadratic	.227	Zero Mean Gaussian
One Cycle Sinusoidal	.114	Rayleigh
Two Cycle Sinusoidal	.058	Rayleigh
Phase Errors(Degrees) **Total Excursion**		
Quadratic	33.1	Zero Mean Gaussian
One Cycle Sinusoidal	8.4	Rayleigh
Two Cycle Sinusoidal	3.3	Rayleigh

Table V
-15 dB Width Measurement Errors (Δ)

		Cosine Weighting		-35 dB Taylor	
		Bias	Std Dev	Bias	Std Dev
Mode A	No System Errors	+8.7	7.7	+1.1	0.0
	System Errors of Table III	+13.9	9.7	+11.1	4.8
	Twice the Errors of Table III	+20.2	17.4	+15.8	12.3
Mode B	No System Errors	+11.0	10.2	+2.1	1.9
	System Errors of Table III	+14.9	9.8	+12.4	5.7
	Twice the Errors of Table III	+22.6	18.4	+18.4	11.9